Research Article | Vol. 27, No. 20 / 30 September 2019 / Optics Express 28523
Optics EXPRESS

High power, single-frequency, monolithic fiber amplifier for the next generation of gravitational wave detectors

FELIX WELLMANN,[1,*] MICHAEL STEINKE,[1] FABIAN MEYLAHN,[2] NINA BODE,[2] BENNO WILLKE,[2] LUDGER OVERMEYER,[1,3] JÖRG NEUMANN,[1] AND DIETMAR KRACHT[1]

[1]*Laser Zentrum Hannover e.V., Hollerithallee 8, 30419 Hannover, Germany*
[2]*Max-Planck-Institut für Gravitationsphysik (Albert-Einstein-Institut) and Leibniz Universität Hannover, Callinstr. 38, 30167 Hannover, Germany*
[3]*Institut für Transport- und Automatisierungstechnik, Leibniz Universität Hannover, An der Universität 2, 30823 Garbsen, Germany*
[*]*f.wellmann@lzh.de*

Abstract: Low noise, high power single-frequency lasers and amplifiers are key components of interferometric gravitational wave detectors. One way to increase the detector sensitivity is to increase the power injected into the interferometers. We developed a fiber amplifier engineering prototype with a pump power limited output power of 200 W at 1064 nm. No signs of stimulated Brillouin scattering are observed at 200 W. At the maximum output power the polarization extinction ratio is above 19 dB and the fractional power in the fundamental transverse mode (TEM_{00}) was measured to be 94.8 %. In addition, measurements of the frequency noise, relative power noise, and relative pointing noise were performed and demonstrate excellent low noise properties over the entire output power slope. In the context of single-frequency fiber amplifiers, the measured relative pointing noise below 100 Hz and the higher order mode content is, to the best of our knowledge, at 200 W the lowest ever measured. A long-term test of more than 695 h demonstrated stable operation without beam quality degradation. It is also the longest single-frequency fiber amplifier operation at 200 W ever reported.

1. Introduction

In 2016, the first direct observation of gravitational waves by interferometric gravitational wave detectors (GWD) was reported [1]. Several further detections, partly confirmed by independent observations in the electromagnetic spectrum [2], led to an increased interest in a new generation of GWDs with increased sensitivity. Several design studies have been compiled [3,4] and propose GWD designs which would open a new range of detectable astrophysical events and enable improved multi-messenger astronomy [2]. One design approach that directly impacts the laser development at 1064 nm, is the operation of the interferometer at room temperature with up to 500 W laser power at 1064 nm [4].

Current state-of-the-art GWDs, e.g., the advanced LIGO (aLIGO) detectors, use solid-state injection-locked Nd:YAG ring oscillators to achieve up to 200 W optical power [5]. These solid-state lasers (SSL) fulfill the power and noise requirements but have disadvantages regarding usability, maintenance procedures and further power scaling. At increased output power levels, these lasers require complex cooling strategies and tend to increased thermal lensing, which leads to instabilities and reduction of beam quality. The output power cannot be freely chosen because the thermal lensing is part of the resonator design and is highly optimized for a pre-defined working point. In addition, a sophisticated cooling system is required to remove approximately 3 kW of heat load during operation.

#370143 https://doi.org/10.1364/OE.27.028523
Journal © 2019 Received 18 Jun 2019; revised 7 Aug 2019; accepted 2 Sep 2019; published 20 Sep 2019

Optics EXPRESS

Fiber technology has been identified as a promising alternative to overcome limitations of the SSL system [6]. Fiber amplifiers enable very high output power levels and fulfill GWD requirements regarding low noise levels and exceptional beam quality (above 90 % TEM_{00}-mode content). They also produce low and well distributed heat load. The fiber amplifier system can be designed to be easily operated and enables simple maintenance procedures, upgrades, and repair. Therefore, high power monolithic fiber amplifiers at 1064 nm that emit a linearly-polarized fundamental TEM_{00}-mode are promising candidates for GWD laser sources. However, the limiting factor for output power scaling of single-frequency fiber amplifiers is stimulated Brillouin scattering (SBS). Besides the output power limiting effect, SBS generates excess high frequency power noise in the MHz range [7] where shot-noise limited performance is necessary for the length and alignment stabilization loops used in GWDs [8].

In recent years, several (monolithic) single-frequency fiber amplifiers have been developed that demonstrated the power scalability of such devices. In 2012, Karow et al. [9] reported a free-space pumped photonic crystal fiber based amplifier with 203 W of output power in the TEM_{00}-mode. Additionally, no noise increase in the MHz range was observed with the conclusion of a truly SBS-free amplifier. Karow et al.[9] also pointed out that the M^2-measurement is insufficient for evaluating the TEM_{00}-mode content, which is the mode currently exclusively used in GWDs. Wielandy [10] investigated the impact of higher order modes on the M^2-measurement and concluded that an $M^2<1.1$ allows for a higher order mode content as high as 30 %. In 2013, Huang et al. [11] demonstrated 414 W output power with an M^2 of 1.34. The single-frequency output power record is held by Robin et al. [12] with an output power of 811 W, an M^2 of 1.2, and 10 % of the output power propagating backwards because of SBS. Most recently, Pierre et al. [13] developed a free-space pumped amplifier that demonstrated 208.6 W with an M^2 of 1.2, no signs of SBS were observed and stable operation for approximately 90 h was reported.

In 2012, Theeg et al. [14] reported a fiber based signal-pump-combiner concept that is currently used in our high power amplifier module. The other necessary fiber component concepts such as the mode field adapter and cladding-light-stripper [15] were also developed in-house. In a first experimental step a fiber amplifier was built, which demonstrated excellent beam quality (94 % TEM_{00}-mode content at 200 W), high polarization extinction ratio (PER) of >20 dB , and a maximum output power of 300 W [16] (approximately 250 W SBS-free). Followed by a concept development in 2018 of an engineering fiber amplifier prototype [17] with increased reliability, modularity and usability. The performance of the engineering prototype is discussed within the remaining sections of this paper.

2. Engineering prototype setup

The fiber amplifier engineering prototype (Fig. 1) consists of three individual modules, the seed-laser module, the first (pre-amplifier) amplifier module, and the second (main-amplifier) amplifier module. The modular design improves the usability, module maintenance, and repair procedures. Each module is spatially separated from the others to further simplify and improve error diagnostics procedures. Besides, in case of a module failure, a pre-assembled module can replace the defective module. The connection between the seed module and the pre-amplifer module is all-fiber and uses a standard single-mode step index fiber. The high power connection between the pre-amplifier module and the main-amplifier module uses a free-space Faraday Isolator (FI) unit between AR-coated ½" fiber end-caps. A plug-in end-cap design enables easy replacement of a module by simply exchanging the associated fiber end-cap in the FI interface unit. The replacements can be done without difficulty and non-standard splices between PM-LMA fibers. Therefore, costly GWD down-times because of laser maintenance or repair can be kept at a minimum.

Optics EXPRESS

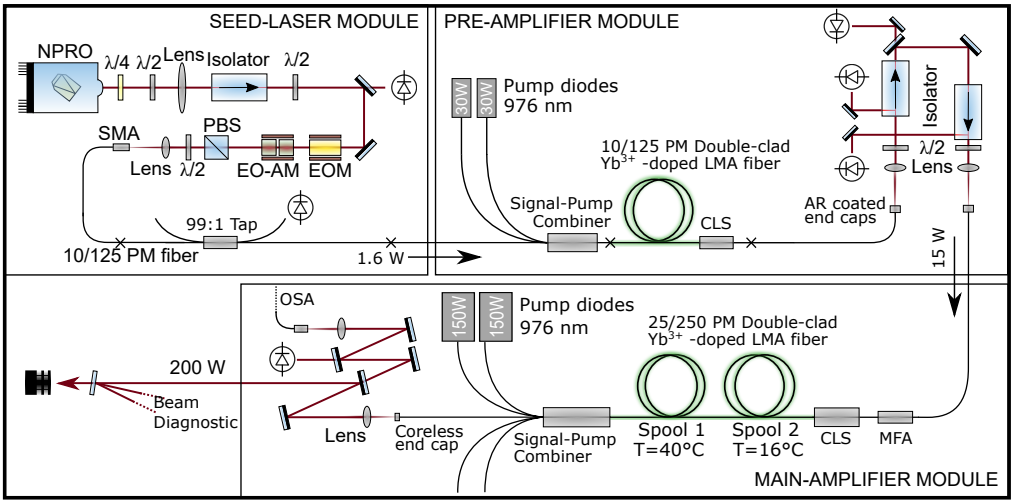

Fig. 1. Setup of the engineering fiber amplifier prototype: The first module contains a low noise non-planar ring oscillator (NPRO) with an output power of 2 W, modulators for stabilization purposes (currently not installed) and a fiber incoupling. The pre-amplifier uses a 10/125 µm Yb^{3+}-doped PM-fiber and seeds the main-amplifier with 15 W. Two optical isolators protect the amplifier from the main-amplifier. The main-amplifier uses a 25/250 µm Yb^{3+}-doped PM-fiber and was tested up to 200 W of output power.

2.1. Seed laser module

The first module comprises a non-planar ring oscillator (NPRO) as seed laser. The particular NPRO seed source technology has proven to be reliable over the last decade and show exceptional power and frequency noise properties (e.g. 1 kHz measured over 100 ms) and reliability. An optical isolator protects the NPRO from back-reflections and optics are in place to mode-match the laser beam into a standard step-index 10/125 µm PM-fiber. The first module also provides the equipment to monitor power fluctuations, variations of the polarization, and houses additional modulators for stabilization purposes. The module provides 1.6 W within the fiber core, which is sufficient to saturate the first amplifier module.

2.2. Pre-amplifier module and connector interface

The pre-amplifier module is based on a 3 m long standard step-index 10/125 µm LMA Yb^{3+}-doped PM-fiber (Nufern PLMA-YDF-10/125-M) and 2.5 m of matched passive 10/125 µm LMA PM-fiber. The active fiber is pumped at 976 nm in a co-propagating configuration. This configuration reduces thermal load at the signal-pump-combiner because the amplified signal does not propagate through the splice usually present in fiber-bundle based signal-pump-combiners. However, the propagation of pump light and signal in the same direction has the disadvantage of a weak pump-induced thermal gradient along the fiber, which decreases the SBS threshold [18]. Any residual pump light is removed by an in-house fabricated cladding light stripper (CLS) which is based on a microstructured cladding [15]. The seed signal is amplified by the pre-amplifier and 15 W is coupled into the fiber of the main-amplifier module.

The pre-amplifier is protected from backward propagating light coming from the main-amplifier by two optical isolators. AR-coated fiber end-caps as shown in Fig. 2 are used as connector interfaces between the free-space optics in the FI unit and the fibers of the monolithic amplifier modules.

Optics EXPRESS

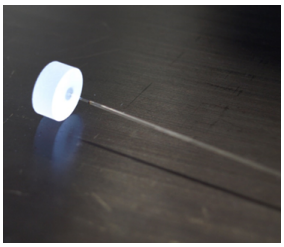

Fig. 2. Fiber fused to an AR coated substrate.

The fibers are directly fused to the substrate using a CO_2-Laser. The splice to the substrate does not degrade the beam quality and is optimized for low losses. These end-caps are designed for high power operation and are kinematically mounted to ensure stable operation and easy replacement. The use of free space components between the two amplifier modules has an advantage regarding the usability and reliability of the system. It also ensures that the total fiber length is at a minimum to avoid the early onset of SBS. The use of well-known and reliable high power optical components ensures stable long-term operation. It also enhances the modular design approach of the entire system because fiber splices between PM-fibers are avoided. As mentioned above, the plug-in end-cap design enables easy replacement of a module by simply exchanging the associated fiber end-cap in the FI interface unit.

2.3. Main-amplifier module

The main-amplifier module is seeded by the pre-amplifier and is counter-propagating pumped at 976 nm. This configuration increases the SBS threshold by a more advantageous thermal gradient along the fiber [19]. However, the thermal load on the combiner increases because the amplified signal in addition to the pump radiation must propagate through the combiner. The fiber amplifier is manufactured out of two types of optical fibers. Approximately 0.3 m passive single mode 10/125 µm PM-fiber is used as an input fiber, which is connected via a mode field adapter to 3 m of standard step-index 25/250 µm Yb^{3+}-doped PM-fiber (Nufern PLMA-YDF-25/250-M). This design ensures a long-term stable excitation of the fundamental mode of the 25/250 µm fiber. Any change of the incoupling, caused by e.g. pointing of the pre-amplifier beam only results in a change of power throughput but does not change the mode-matching to the core of the 25/250 µm fiber. In addition, the splice between the 10 µm and 25 µm fiber is the only fiber splice of the entire high-power fiber amplifier section. The other fiber components such as the pump light stripper and the signal-pump-combiner are manufactured using the active fiber [15]. The pump fibers of the signal-pump-combiner are side fused and therefore eliminate the need for a splice at the point with the highest optical power load [14].

3. Optical properties and long-term operation

The main-amplifier module is capable of delivering 200 W of optical power. Figure 3 shows the slope as the output power vs. total pump power and does not include coupling losses of 8 % ± 2 % within the combiner and approximately 3.5 % residual pump light removed by the CLS (assuming the specified cladding light attenuation of 5.1 dB m^{-1} at 975 nm). The slope efficiency above 100 W pump power is calculated via a linear fit to be 75 %. The low efficiency at amplifier output power levels below 40 W is caused by the pump's central wavelength being shifted away from the absorption maximum of Yb^{3+} at 976 nm. The pump diodes are designed to achieve a central wavelength of 976 nm at high output powers (>100 W). A compensation at low output powers by changing the diode temperature is only partially possible.

Optics EXPRESS

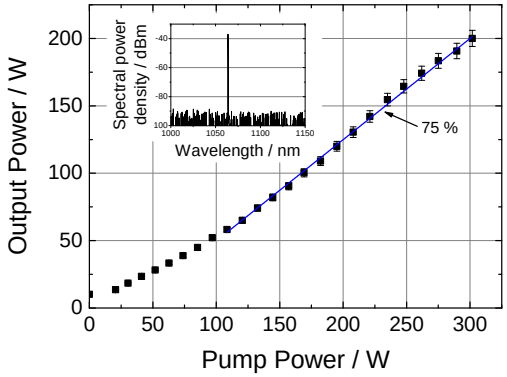

Fig. 3. Amplifier slope up to a pump-limited maximum output power of 200 W. Inset: Optical spectrum shows >50 dB signal to amplified spontaneous emission (ASE) suppression at 200 W output power (0.01 nm measurement resolution).

3.1. Long-term operation

The system was operated at 204 W in total for approximately 695 h, thereof 550 h without any interruptions. To the best of our knowledge, this corresponds to the longest operation of a single-frequency fiber amplifier with an output power of >200 W. A third pump diode enabled output power levels above 200 W. At the beginning of the measurement, multiple on/off cycles were performed while during every cycle thermal equilibrium was reached in less than 1 h of operation. The thermal cycling did not influence the performance of the amplifier. After the power cycling, an average output power during the long term test was calculated as 204.17 W ± 1.76 W (relative standard deviation: <1%). During the operation, a degradation of the beam shape could be observed, which also resulted in a observed power decrease. Figure 4 shows the decrease as a slow power drop over 300 h of approximately 4 % beginning at 150 h. The degradation was related to the mechanical instability of the core-less fiber end-cap in relation to the out-coupler lens. A mechanical readjustment of these components retrieved the initial performance (c.f. Figure 5). A minor improved mechanical setup is needed for a second iteration of the amplifier to overcome this stability issue.

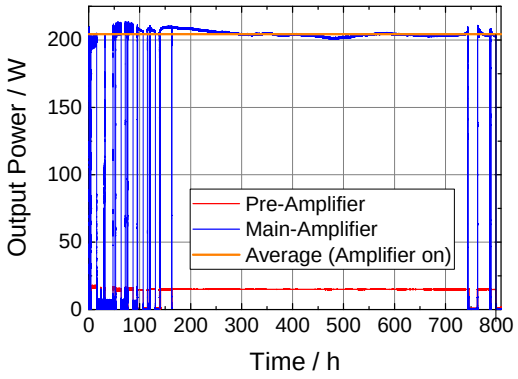

Fig. 4. Long-term test of the fiber amplifier at 204 W output power. During the first 150 h, multiple on/off cycles were performed and no degradation of the performance was observed. In total the amplifier was operated for 695 h.

Optics EXPRESS

3.2. Beam quality and polarization extinction ratio

A pure TEM_{00}-mode and linearly polarized beam is required for GWDs. Wrong polarized light or any higher order modes are removed by polarizing optics and a mode-cleaner cavity before the beam is coupled into the interferometer. Therefore, the modal composition of the output beam is analyzed and the usable TEM_{00}-mode content is calculated. As explained, the M^2-measurement is not sufficient to estimate the higher order mode content because even an $M^2<1.1$ can contain up to 30 % higher order modes [10].

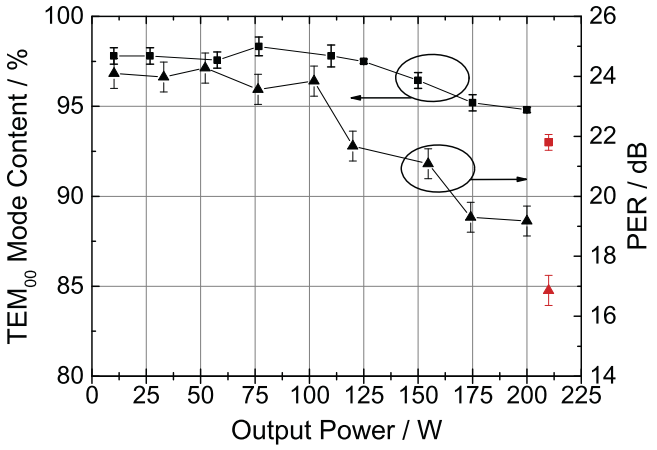

Fig. 5. TEM_{00}-mode content remains at approx. 97.5 % up to 125 W and decreases to 94.8 % at 200 W. The PER shows a similar behaviour decreasing from 24 dB at up to 100 W down to 19 dB at 200 W. After 650 h of operation the higher order mode content is measured at 208 W to be 7 % and the PER of 17 dB (both measurements shown in red).

The modal composition of the output beam and the fundamental TEM_{00}-mode content was analyzed with a non-confocal scanning ring cavity as described by Kwee et al. in [20]. The eigenmodes of such a ring cavity correspond to the TEM-modes of the same order. Thus, scanning the cavity over a free spectral range allows measuring the relative TEM_{00}-mode content and the higher order mode content. Figure 5 shows the TEM_{00}-mode content over the entire output power slope. Up to an output power of 125 W the fundamental mode content is measured to be higher than 97.5 % and decreases to 94.8 % at the maximum output power. In terms of single-frequency amplifiers and laser it is, to the best of our knowledge, the highest TEM_{00}-mode content ever measured at a power level of 200 W. Figure 5 shows a stable polarization extinction ratio (PER) of approximately 24 dB up to 100 W. The PER reduces down to 19 dB up to the maximum output power. These excellent optical properties are achieved by the integration of the pump combiner [12], the CLS and the mode field adapter directly using the active fiber. Therefore, additional splices have been avoided, which are usually the reason for a reduced PER and beam quality degradation. No signs of transverse mode instabilities could be observed during operation. After 650 h of operation the TEM_{00}-mode content and the PER was measured again to evaluate potential degradation of the fiber or fiber components. These measurements are shown in Fig. 5 in red and were performed at 208 W. The higher order mode content was measured to be 7 %. However, the beam quality measurement method only provides a lower limit of the TEM_{00}-mode content and the difference between the initial beam quality measurements was only limited by the mode-matching to the measurement cavity. In conclusion, the beam quality was not significantly affected by the long-term operation. The PER was also measured at 208 W to be 17 dB. The PER measurement showed a slight degradation of 2 dB, which results in an additional

Optics EXPRESS

unusable power in the wrong polarization of approximately 1.5 W. These values are very close to the initial measurements and indicate that a stable operation for many months is possible.

3.3. Suppression of stimulated Brillouin scattering

The main limitation of single-frequency fiber amplifiers is SBS, which results in an increased power propagating in the opposite direction of the signal. The SBS-threshold can be increased by applying a thermal gradient on the fiber additionally to the pump-induced intrinsic thermal gradient. Thereby, the SBS gain spectra of the fiber sections are separated, which results in a higher SBS threshold [21]. The SBS gain spectrum experiences a frequency shift of 2.25 MHz K^{-1} [18] and therefore a temperature difference of $\Delta T = 24$ K results in a sufficient separation of the two gain spectra. This method is implemented by using two fiber spools at different temperatures as shown in Fig. 1. Approximately 1/3 of the last section of the active fiber is heated to 40 °C while the other part of the fiber is cooled to 16 °C. Theeg et al. [16] investigated the SBS suppression design of a prior version of the amplifier. The lower temperature limit is defined by the dew point of the lab environment and the maximum temperature by the heat resistance of the polymer coating. Although, the SBS suppression by applying an additional thermal gradient is easy to implement and operate it has the minor disadvantage of a slight increased initial switch-on time of a few minutes that is necessary to let the fiber spools reach the desired temperatures.

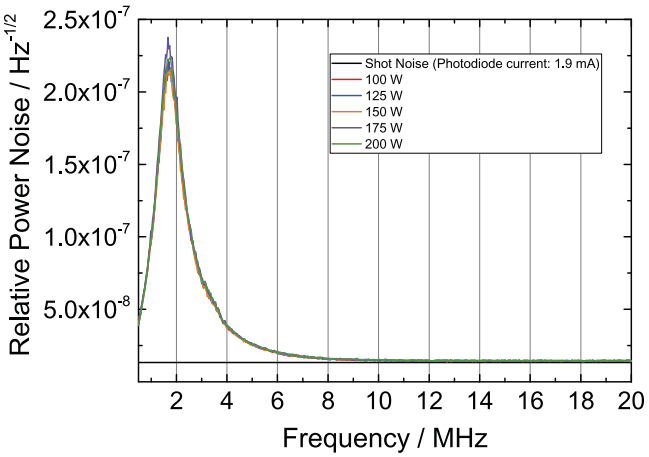

Fig. 6. HF amplitude spectral density of the power noise at several amplifier output power levels. No excess noise was observed. The photodiode current is 1.9 mA at all measurements. The fiber spool temperature (c.f. Figure 1) difference is $\Delta T = 24$ K.

SBS also generates high frequency power noise in the MHz range [7]. In GWDs the MHz frequency range is used for length and alignment stabilization purposes via imprinted modulation side bands and requires low power noise performance of the laser source at these frequencies [8]. In comparison with the commonly used SBS detection method of monitoring the backward propagating power, the method of monitoring the high frequency (HF) relative power noise is the most sensitive SBS detection method [18]. Therefore, the relative power noise was measured in the frequency range from 500 kHz to 20 MHz and at several output power levels as shown in Fig. 6. The photodiode current is constant at I = 1.9 mA at all power levels. A low shot-noise level is achieved by adjusting the optical power on the photodiode to be as high as possible without saturating it. The measurement shows shot-noise limited performance at the maximum output power. No signs of SBS could be observed. The peak at approximately 1 MHz corresponds to the relaxation oscillation frequency of the NPRO. The NPRO is operated in the single-frequency

Optics EXPRESS

regime and away from a mode-hop regime where two modes can oscillate within its resonator crystal.

4. Optical noise properties

In addition to the PER, beam quality properties, and HF power noise, several other noise properties have been characterized with respect to the requirements of GWDs in the frequency range of 1 Hz to 100 kHz. This includes the frequency noise, the relative power noise, and the relative pointing noise. The diagnostic breadboard (DBB) device described by Kwee et al. in [20] is used to perform these measurements. As mentioned, the NPRO is operated in the single-frequency regime and away from a mode-hop regime where two modes can oscillate within its resonator crystal.

4.1. Frequency noise

Figure 7 shows frequency noise measurements at several output power levels. The measurements are performed by stabilizing the beam to the fundamental mode of the DBB's ring cavity. One mirror of the cavity is mounted on a piezo and allows adjustments to keep the beam resonant. The frequency noise is calculated using the error and control signal of the feed-back control loop [20].

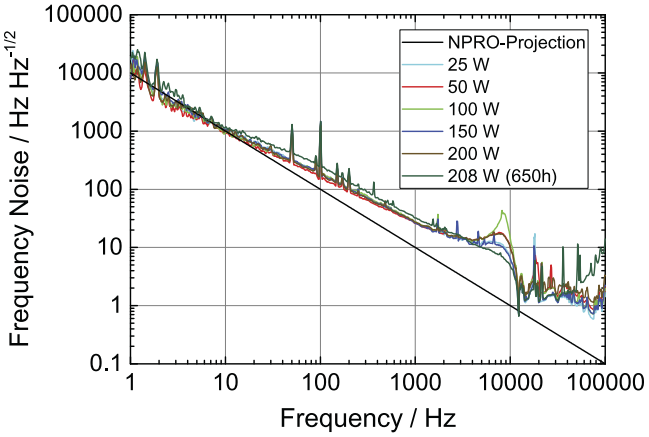

Fig. 7. Frequency noise measurements at several amplifier output power levels. The measurements show no relevant increase in frequency noise. The feature at around 8 kHz is caused by the feedback loop of the measurement setup. The NPRO frequency noise projection is shown as reference.

The measurement shows that the frequency noise is nearly unaffected in a range from 1 Hz to 100 kHz at all output power levels. The measured frequency noise performance is at all power levels in line with the necessary noise properties required for the use in GWDs. The peak at approximately 8 kHz is related to the feedback loop of the ring cavity. The typical NPRO frequency noise behavior is plotted as a reference. Amplified spontaneous emission (ASE) can be the reason for increased frequency noise. However, the inset of Fig. 3 shows 50 dB suppression of signal to ASE in addition to the stable frequency noise performance up to 200 W. The frequency noise measurement was repeated at an output power of 208 W after operating the amplifier above 200 W for 650 h. The measurement shows no significant deviations from the initial measurements.

Optics EXPRESS

4.2. Relative power noise

Additionally to the HF relative power noise shown in Fig. 6, the relative power noise in the frequency range from 1 Hz to 100 kHz is relevant for gravitational wave detection. The relative power noise (Fig. 8) was analyzed at several power levels up to 200 W. Figure 8 shows the free-running laser system; a power stabilization can be realized by e.g. pump power modulation as demonstrated by Thies et al. [22].

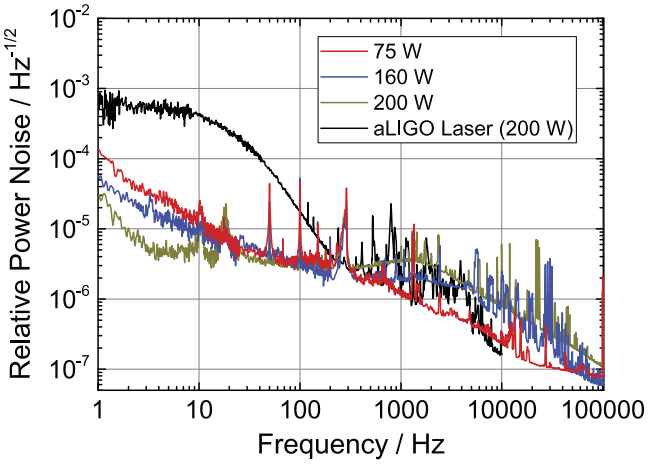

Fig. 8. Relative power noise measurements at several amplifier output power levels in comparison with the 200 W solid-state laser used in the aLIGO detectors (data from [23]). At low frequency the noise is dominated by the current noise of the pump laser diode driver. At higher frequencies the noise is dominated by the seed laser.

The relative power noise experiences some variations while the output power of the amplifier increases. Below approximately 30 Hz a decrease of the noise was observed, which is related to pump temperature stability issues at lower output power levels. At frequencies above 1 kHz, the noise level increases which is caused by increasing noise contribution of the pumps. The reason therefore is the low pass corner frequency shift to higher frequencies of the transfer function of pump to output signal [24]. However, the relative power noise is at all power levels suitable for the use in GWDs. The noise properties are compared to the measurements of the 200 W SSL-system at the aLIGO Hanford Observatory [23]. The fiber amplifier relative power noise shows lower noise of up to one order of magnitude in the frequency range from 1 Hz to 200 Hz. At higher frequencies above 10 kHz the relative power noise is determined by the seed source, which is comparable to the SSL-system.

4.3. Relative pointing noise

The stability of the beam pointing is crucial to achieve low noise performance. As explained, the output beam of the laser passes through a mode-cleaner ring cavity to remove higher order mode content before it is coupled into the GWD's interferometer. Beam pointing at the input of a mode-cleaner is transferred into power noise at its output and must therefore be kept as low as possible. The DBB is used to evaluate the amplifier pointing performance. The DBB uses its ring cavity, which is stabilized to its fundamental mode, as pointing reference. Figure 9 shows the measurements as RMS value of X and Y pointing measurements. The pointing noise is analyzed at several output power levels and shows degradation up to the maximum output power of 200 W. This behavior is related to increased contribution of higher order modes to the beam, which appears as beam pointing during the measurement. In comparison to the SSL-system the

Optics EXPRESS

pointing noise of the fiber amplifier beam is lower up to approximately 100 Hz. In this frequency range, the fiber amplifier pointing noise performance is up to two orders of magnitude lower. At higher frequencies the noise is comparable. The low frequency relative pointing noise, up to approximately 100 Hz is at 200 W, to the best of out knowledge, the lowest ever reported.

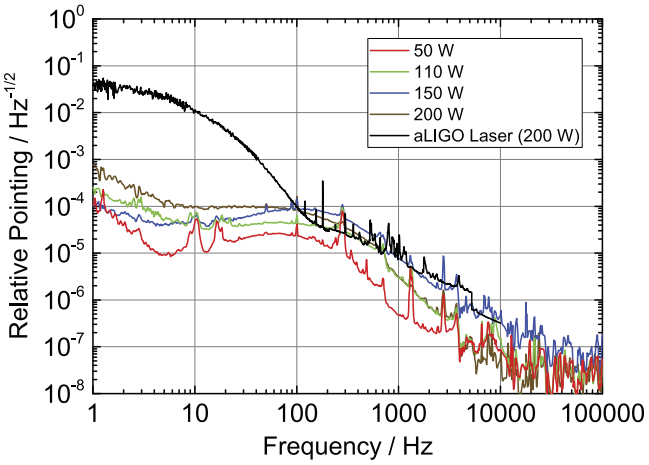

Fig. 9. Relative pointing noise spectra at several output power levels. The measurements are compared to the relative pointing noise measurements of the 200 W SSL (data from [23]). The pointing noise is exceptionally low at frequencies below 100 Hz.

5. Conclusion

Single-frequency fiber amplifiers are promising laser sources to address the challenging requirements of the next-generation GWDs. Monolithic amplifier can be compact, reliable, easy to operate, and simple to maintain. We developed a monolithic PM-LMA Yb^{3+}-doped high power fiber amplifier module using a standard step-index fiber with a 25 µm core diameter. The fiber amplifier system has a pump power limited output power of 200 W with a TEM_{00}-mode content of 94.8 % and a PER above 19 dB. The frequency noise, relative power and pointing noise spectra were analyzed and demonstrated excellent noise properties. The measured noise properties are at all power levels suitable for the use in GWDs. No signs of SBS were observed. The amplifier was operated for approximately 695 h, thereof 550 h without interruption at >200 W and demonstrated stable operation.

Funding

Max-Planck-Gesellschaft.

Acknowledgments

We would like to thank Thomas Theeg from FiberBridge Photonics GmbH for the ongoing and successful cooperation in the field of fiber component technology.

References

1. B. P. Abbott, *et al.* (LIGO scientific collaboration and Virgo collaboration), "Observation of gravitational waves from a binary black hole merger," Phys. Rev. Lett. **116**(6), 061102 (2016).
2. B. P. Abbott, *et al.* (LIGO scientific collaboration and Virgo collaboration), "Multi-messenger observations of a binary neutron star merger," Astrophys. J. Lett. **848**, L12 (2017).
3. LIGO Science Collaboration, "Exploring the Sensitivity of Next Generation Gravitational Wave Detectors," Classical Quantum Gravity **34**, 044001 (2017).

Optics EXPRESS

4. M. Abernathy, *et al.*, "Einstein Gravitational Wave Telescope Conceptual Design Study," European Gravitational Observatory Document ET-0106A-10 (2011).
5. L. Winkelmann, O. Puncken, R. Kluzik, C. Veltkamp, P. Kwee, J. Poeld, C. Bogan, B. Willke, M. Frede, J. Neumann, P. Wessels, and D. Kracht, "Injection-locked single-frequency laser with an output power of 220 W," Appl. Phys. B: Lasers Opt. **102**(3), 529–538 (2011).
6. M. Steinke, H. Tünnermann, V. Kuhn, T. Theeg, M. Karow, O. de Varona, P. Jahn, P. Booker, J. Neumann, P. Weßels, and D. Kracht, "Single-Frequency Fiber Amplifiers for Next-Generation Gravitational Wave Detectors," IEEE J. Select. Topics Quantum Electron. **24**(3), 1–13 (2018).
7. J. Zhang and M. R. Phillips, "Modeling Intensity Noise Caused by Stimulated Brillouin Scattering in Optical Fibers," *Conf. Laser Electr.*, 140–142 (2005).
8. K. Izumi and D. Sigg, "Advanced LIGO: Length Sensing and Control in a Dual Recycled Interferometric Gravitational Wave Antenna," Classical Quantum Gravity **34**(1), 015001 (2017).
9. M. Karow, C. Basu, D. Kracht, J. Neumann, and P. Weßels, "TEM_{00} Mode Content of a Two Stage Single-Frequency Yb-doped PCF MOPA with 246 W of Output Power," Opt. Express **20**(5), 5319–5324 (2012).
10. S. Wielandy, "Implications of Higher-Order Mode Content in Large Mode Area Fibers with Good Beam Quality," Opt. Express **15**(23), 15402–15409 (2007).
11. L. Huang, H. Wu, R. Li, L. Li, P. Ma, X. Wang, J. Leng, and P. Zhou, "414 W Near-Diffraction-Limited all-Fiberized Single-Frequency Polarization-Maintained Fiber Amplifier," Opt. Lett. **42**(1), 1–4 (2017).
12. C. Robin, I. Dajani, and B. Pulford, "Modal Instability-Suppressing, Single-Frequency Photonic Crystal Fiber Amplifier with 811 W Output Power," Opt. Lett. **39**(3), 666–669 (2014).
13. C. Pierre, G. Guiraud, J. Yehouessi, G. Santarelli, J. Boullet, N. Traynor, and C. Vincont, "200-W Single Frequency Laser based on Short Active Double Clad Tapered Fiber," Proc. SPIE **10512**, 105122A (2018).
14. T. Theeg, H. Sayinc, J. Neumann, L. Overmeyer, and D. Kracht, "Pump and Signal Combiner for Bi-Directional Pumping of all-Fiber Lasers and Amplifiers," Opt. Express **20**(27), 28125–28141 (2012).
15. M. Wysmolek, C. Ottenhues, T. Pulzer, T. Theeg, H. Sayinc, M. Steinke, U. Morgner, J. Neumann, and D. Kracht, "Microstructured Fiber Cladding Light Stripper for Kilowatt-Class Laser Systems," Appl. Opt. **57**(23), 6640–6644 (2018).
16. T. Theeg, H. Sayinc, J. Neumann, and D. Kracht, "All-Fiber Counter-Propagation Pumped Single Frequency Amplifier Stage With 300-W Output Power," IEEE Photonics Technol. Lett. **24**(20), 1864–1867 (2012).
17. F. Wellmann, P. Booker, S. Hochheim, T. Theeg, O. de Varona, W. Fittkau, L. Overmeyer, M. Steinke, P. Weßels, J. Neumann, and D. Kracht, "Recent Progress on Monolithic Fiber Amplifiers for Next Generation of Gravitational Wave Detectors," Proc. SPIE **10512**, 105120I (2018).
18. M. Hildebrandt, S. Büsche, P. Weßels, M. Frede, and D. Kracht, "Brillouin Scattering Spectra in High-Power Single-Frequency Ytterbium Doped Fiber Amplifiers," Opt. Express **16**(20), 15970–15979 (2008).
19. V. I. Kovalev and R. G. Harrison, "Suppression of Stimulated Brillouin Scattering in High-Power Single-Frequency Fiber Amplifiers," Opt. Lett. **31**(2), 161–163 (2006).
20. P. Kwee, F. Seifert, B. Willke, and K. Danzmann, "Laser Beam Quality and Pointing Measurement with an Optical Resonator," Rev. Sci. Instrum. **78**(7), 073103 (2007).
21. A. Liu, X. Chen, M. J. Li, J. Wang, D. T. Walton, and L. A. Zenteno, "Comprehensive Modeling of Single Frequency Fiber Amplifiers for Mitigating Stimulated Brillouin Scattering," J. Lightwave Technol. **27**(13), 2189–2198 (2009).
22. F. Thies, N. Bode, P. Oppermann, M. Frede, B. Schulz, and B. Willke, "Nd:YVO4 High-Power Master Oscillator Power Amplifier Laser System for Second-Generation Gravitational Wave Detectors," Opt. Lett. **44**(3), 719–722 (2019).
23. B. Willke, *et al.*, "Pre-Stabilized Laser Subsystem Testing and Acceptance - L1 PSL(LIGO scientific collaboration)," Technical Report No. LIGO-E1100716-v6, (2012) https://dcc.ligo.org/LIGOE1100716/public.
24. H. Tünnermann, J. Neumann, D. Kracht, and P. Weßels, "Gain Dynamics and Refractive Index Changes in Fiber Amplifiers: a Frequency Domain Approach," Opt. Express **20**(12), 13539–13550 (2012).